Comparing Measured and Computed Nonlinear Frequency Responses to Calibrate Nonlinear System Models

Michael W. Sracic
Postdoctoral Research Associate
mwsracic@gmail.com

Shifei Yang
Graduate Research Assistant
University of Wisconsin-Madison
syang66@wisc.edu

&
Matthew S. Allen
Assistant Professor
msallen@engr.wisc.edu
Department of Engineering Physics
University of Wisconsin-Madison
535 Engineering Research Building
1500 Engineering Drive
Madison, WI 53706

ABSTRACT

Many systems of interest contain nonlinearities that are difficult to accurately model from first principles, so it would be preferable to characterize the system experimentally. For many nonlinear systems, it is now possible to measure frequency response curves with stepped sine testing and to compute frequency response curves with numerical continuation. Nonlinear frequency response curves are very sensitive to the system model and the nonlinearities and they provide a lot of insight into the response of the system to a variety of inputs. This paper explores the feasibility of a nonlinear model updating approach based on nonlinear frequency response and the experimental and analytical tools that are needed. For the experiment, a cantilever beam with an unknown nonlinearity is driven with a harmonic force at various frequencies. The steady-state response is measured and processed with the fast Fourier transform to obtain the frequency response curve. Some subtle yet important details regarding how this is implemented are discussed. An analytical model is also constructed and its frequency response computed using a recently developed technique. The measured and simulated frequencies are then compared and used to tune the analytical model.

1. Introduction

The frequency response function has long been used to characterize the dynamic response of linear systems. For nonlinear systems, the nonlinear frequency response has also proven very useful, even with the additional complexities that are introduced. Several different approaches have been taken to calculate frequency response from a known mathematical model. A few studies combine the Harmonic Balance Technique with a numerical continuation algorithm to compute the frequency response curves of torsional sub-systems with clearance nonlinearities [1] or nonlinear mesh phase interactions in multi-gearbox drive systems [2]. This method is a semi-analytical approach since it uses the HBM formulation and closed-form equations of motion. In another paper [3], Padmanabhan and Singh used a purely numerical approach based on shooting methods to compute nonlinear

frequency response curves and to characterize jump phenomena, subharmonic responses, and chaos. However, as they discuss in [3], the algorithm seems to break down for higher-order nonlinear systems. Ribeiro also used a numerical shooting approach to study frequency responses of geometrically nonlinear beams and plates [4], but the algorithm used in that study doesn't appear to be equipped to follow turning points [5] on branches that lead to unstable periodic solutions. Finally, Gibert [6] used a numerical continuation approach based on nonlinear normal modes (NNMs) to compute the nonlinear frequency responses of a beam model, and then used model updating method to match those frequency responses to an actual beam. However, his method requires one to choose a specific number of NNMs to use in the calculation, and this approximation may break down for certain nonlinearities or if an insufficient number of nonlinear normal modes is used.

In this paper, the numerical algorithm presented by the authors in [7] is used to calculate nonlinear frequency responses. The algorithm is based on shooting and continuation techniques that are very similar to those used in [8] to find the nonlinear normal modes of unforced systems. Here, the system is excited with a sinusoidal input force and the response is found over one period of the excitation. The initial conditions are then adjusted until a steady state response is obtained and numerical continuation techniques are used to calculate a branch of periodic responses for different forcing frequencies (i.e. essentially a frequency response). The algorithm used in this work is identical to the one presented in [7] except that in this work the Jacobians that are required were computed numerically using finite differences, so the equations of motion do not need to be known in closed form.

Once a model has been formed and its frequency response has been calculated, one can use experiments to validate and update the model. In the paper by Ribeiro [4] this was done by calculating one nonlinear frequency response and comparing it to a measured frequency response near one of the beam's resonances. In [9], Carella and Ewins measure nonlinear frequency response a system using a stepped-sine testing approach and extract a first order approximation (linear) model for specific forcing amplitudes. This approach though is applied to a single mode of the system and doesn't seem to consider any higher harmonic information associated with the nonlinearity. In [6], Gibert compares frequency responses between an analytical model of a beam and an actual beam near three resonances, and in this paper a similar approach will be employed. A cantilever beam was constructed in the laboratory, and a geometric stiffness nonlinearity was created by attaching a small strip of nylon between the beam's free end and a fixture. The nonlinear frequency response was then estimated using stepped-sine excitation. A numerical model of the beam was constructed using a Ritz-Galerkin approach and its frequency responses were computed using a numerical continuation approach and compared to the measured frequency responses of the actual beam. The information from the frequency responses and from the harmonic information contained in the periodic time history responses are used to evaluate the accuracy of the model, and some initial is made to update the model to correctly capture the beam's dynamics.

The methods used in this paper should be applicable to a broad range of systems. The nonlinear frequency response of a system can be computed over a wide range of frequencies using efficient shooting and continuation techniques [3, 7, 8] and they are not reliant on any approximation, such as an assumed number of polynomial terms approximating the nonlinearity. The resulting nonlinear frequency responses can be readily compared to measurements, paralleling the way in which linear finite element models are sometimes validated by comparing their linear frequency response functions with measured ones [10].

2. Theoretical Development

Generally, a forced nonlinear system can be represented in state space with the following equation

$$\dot{x} = f\left(x, u\right) \tag{1}$$

where f is a function that describes how the time-dependent state of the system, $x(t)$, and the time-dependent inputs applied to the system, $u(t)$, influence the dynamics of the system. The output response of the system $y(t)$ is often simply a subset of the states, but in general it can be a general nonlinear function of the state and input as follows.

$$y = h\left(x, u\right) \tag{2}$$

When the nonlinear system is subjected to a periodic input with period T (i.e. $u(t+T) = u(t)$), the state and output will often be periodic with $x(t+T) = x(t)$ and $y(t+T) = y(t)$. (In the most general case, the nonlinear system may respond with a longer or shorter period or may respond chaotically even in the presence of periodic input [5, 11], but these issues will not be addressed in this paper.) Thus, it shall be assumed that the period of the forcing will always equal the period of the response. It is more convenient to work with frequencies rather than periods, $\omega_T = (2\pi)/T$, so they will be used in place of the period in the rest of this paper.

2.1   Frequency Response Attributes

The nonlinear frequency response curves describe how the periodic response(s) of a nonlinear system change as the input frequency is varied. For linear systems this is captured by the frequency response function, which relates the magnitude and phase of the input to that of the output. Each point on the frequency response function curve describes a periodic orbit γ, which is a trajectory in the state space that contains the state $\bar{x}$ for every time t. A linear FRF typically has a large magnitude peak near each natural frequency corresponding to high amplitude periodic orbits in the state space. Similarly, the nonlinear frequency response has resonance peaks near its nonlinear normal mode frequencies [12], but there are a few other important differences. Resonance peaks in nonlinear systems can occur away from the nonlinear normal modes (e.g. superharmonic resonances [5]), resonance peaks can contain multi-valued regions where several periodic orbits are possible for single forcing frequencies, certain branches on the nonlinear frequency response curve may contain unstable periodic responses, and finally the law of superposition does not hold for nonlinear systems so frequency responses cannot be linearly scaled when the input amplitude is scaled. Based on the latter point, a nonlinear frequency response is defined by the response alone (i.e. there is no scaling by the input such as in the linear frequency response), and it is only valid for a specific forcing function and amplitude.

Using some of the previous facts, nonlinear frequency response curves can be built from time domain periodic responses, and it is advantageous to have time domain signals because they contain more information about the nonlinearity in the system. For example, consider the Duffing oscillator equation of motion with $\omega_1 = 1$, $\omega_3 = 0.5$, and sinusoidal forcing at a frequency $\omega_T = 1$.

$$\ddot{x} + 0.02\dot{x} + \omega_1^2 x + \omega_3^2 x^3 = \sin(\omega_T t) \tag{3}$$

The response of this system to initial conditions $[x, \dot{x}] = [-0.056, 1.594]$ is periodic. The displacement is plotted over five cycles of the response in Fig. 1(a), and the signal appears to be sinusoidal. The magnitude of the frequency spectrum of this response is plotted in Fig. 1(b) revealing that this is not a pure sinusoid but that there are several frequencies present at 1, 3, 5, etc rad/s (labeled with open circles). The magnitude of these frequency components diminishes with increasing frequency. There are also sharp peaks that rise above the noise floor at 2, 4, 6, etc rad/s.
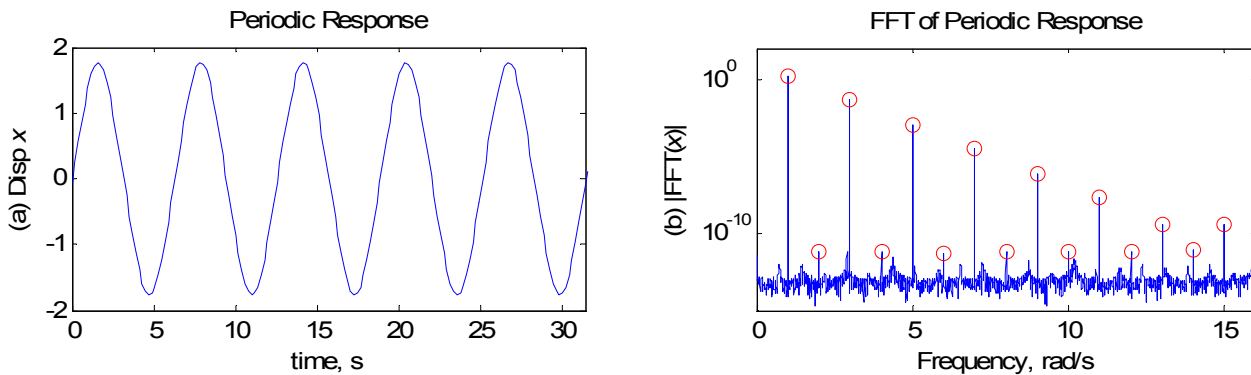

Fig. 1 Periodic time domain response and frequency domain response of the Duffing system

The system is clearly nonlinear since the input was a single frequency sinusoid, yet the system responded at several different frequencies. In particular, if the forcing frequency is designated as the m=1 harmonic then the

odd harmonics of the system (i.e. the m=3, 5, ...) designate peaks at 3 rad/, 5 rad/s, etc. The even harmonics also appear in the spectrum at 2 rad/s, 4 rad/s, etc, however, those peaks are more than ten orders of magnitude smaller than the dominant peak and may be the result of numerical integration error. The harmonic information can be used to build a single point on the frequency response curve. For example, one could record the amplitude of a certain harmonic term in the response for a number of different forcing frequencies and then plot the magnitude of that harmonic term versus the forcing frequency. In some cases a harmonic other than the m=1 (i.e. the driving frequency) harmonic might dominate the responses, so it might be beneficial to choose a harmonic other than the driving frequency. One can also sum the complex amplitudes of all the harmonics at each driving frequency and then plot the magnitude of the sum of the harmonics versus the forcing frequency. No matter which method is chosen, one needs to repeat this process for each stable periodic response on the frequency response curve.

2.2 Simulated Frequency Responses

Numerical continuation techniques can be used to efficiently calculate all of the periodic responses of a system over a wide forcing frequency range. In this paper, a Newton-Raphson correction technique is used to solve the following two-point boundary value problem.

$$H(x,T) = x(T) - x(0) = 0 \tag{4}$$

In particular for a system that is forced at the frequency $\omega_T = (2\pi)/T$, if the response vector $x(T)$ is equal to the initial condition vector $x(0)$, then the response is periodic. This solution provides a single point on the frequency response curve. Once a solution has been established, the following system of equations can be solved to make a prediction for the next solution on the curve.

$$\left[\frac{\partial H}{\partial x}\bigg|_{(x(T),T)} \quad \frac{\partial H}{\partial T}\bigg|_{(x(T),T)} \right]\{P\} = \{0\}$$

$$\{P\} = \left[P_x^{\mathrm{T}} \ P_T \right]^{\mathrm{T}} \tag{5}$$

The Jacobian matrices $\left[\partial H/\partial x\right]$ and $\left[\partial H/\partial T\right]$ can be calculated using closed form equations of motion and the methods described in [7, 13] or by using numerical integration and finite difference equations. In this paper, the latter method is used. The vector P is in the null space of the matrix defined by the Jacobian matrices, so it is tangent to the frequency response curve by construction [7, 8]. Once P has been calculated, it can be used to calculate the initial conditions for the prediction of the next periodic response: $x_{j+1}(0) = x_j(0) + sP_x$ and $T_{j+1} = T_j + sP_T$, where j=0 defines the first periodic solution (i.e. j=0,1,2,3,...) and s is a step-size parameter which can be automatically changed to increase the efficiency of the calculations [7, 8]. The new prediction may need to be corrected so that Eq. (4) is satisfied. Therefore, corrections can be calculated from the following system of equations.

$$\begin{bmatrix} \frac{\partial H}{\partial x}\bigg|_{\left(x_{(j+1)}^{(k)},T_{(j+1)}^{(k)}\right)} & \frac{\partial H}{\partial T}\bigg|_{\left(x_{(j+1)}^{(k)},T_{(j+1)}^{(k)}\right)} \\ \{P_z\}^{\mathrm{T}} & P_T \end{bmatrix} \begin{Bmatrix} \Delta x_{(j+1)}^{(k)} \\ \Delta T_{(j+1)}^{(k)} \end{Bmatrix} = \begin{Bmatrix} -H\left(x_{(j+1)}^{(k)},T_{(j+1)}^{(k)}\right) \\ 0 \end{Bmatrix} \tag{6}$$

The solutions of the previous system have been constrained to be orthogonal to the tangent prediction vector. This was enforced to increase the convergence rate of the calculations. The variable k is used to track the number of corrections that are required until the Eq. (4) has converged. In this paper, the solution has converged when $\left\| H(x,T) \right\| < \left\| x(0) \right\| * 10^{-6}$. The prediction-correction process is repeated for each periodic response within a desired forcing frequency range.

These equations were incorporated into an algorithm that calculates the entire frequency response curve over a large frequency range for one forcing amplitude. The algorithm is automated and efficient, and can be used for relatively high order systems.

3.   Measuring Frequency Response Curves

Swept sine tests are often used to measure the frequency response of linear systems. A similar approach can be used for nonlinear systems; the frequency of the forcing signal is changed step by step in the tests, while the forcing amplitude is the same for all the forcing frequencies. Then, the system's response at each forcing frequency is measured and the nonlinear frequency response curves for this specific forcing amplitude can be constructed within the tested frequency range.

However, there are some important differences between swept sine tests for linear and nonlinear systems. A nonlinear system generally has different frequency response curves for different forcing amplitudes. Furthermore, even with a fixed forcing amplitude, as implied earlier, the system may have several periodic orbits in some frequency ranges. The higher energy periodic orbits are often less stable, so when increasing/decreasing the forcing frequency the system may jump to a lower energy orbit when a disturbance occurs, making the high energy branch more difficult to capture. The high energy branch often contains some of the most valuable information, so it is desirable to capture as much of that branch as possible. Therefore, it is necessary to keep the forcing amplitude constant during the whole test. Sometimes the force can be monitored and controlled to reject disturbances or fluxuations by using a feedback control algorithm [9].

In this work, a National Instrument PXI system was used to generate the step-sine forcing signal and to acquire the responses. A LabView program was designed to generate a continuous forcing signal that has a fixed number of samples per period, ensuring that zero amplitude is obtained at the beginning and the end of each period. Because there are a fixed number of samples per period, the generation rate of the forcing signal varies with the forcing frequency (or the period). When the forcing frequency is stepped, the program waits until the end of a period (i.e. when the amplitude is zero) to change the frequency so that the transient response (disturbance) incurred to the system is minimized. The input force and the response are monitored and the responses are recorded with a fixed sampling rate after the transient responses disappear. At each forcing frequency, the data acquisition program waits prescribed amount of time (typically a few seconds) for the response to reach steady state prior to recording the response and exporting the time series to Matlab for analysis. The magnitudes of the response versus frequency can then be computed using the procedure described in Section 2.1.

4.   Updating models using Nonlinear Frequency Response Curves

Although nonlinear frequency response curves can be substantially more complicated than linear FRFs, general dynamics principles can still be used to interpret the curves. Figure 2 shows several frequency response curves of the Duffing system in Eq. (3), which were calculated using the numerical continuation technique that was summarized previously. The results are plotted in terms of the magnitude of the periodic displacement. For each curve, a different set of values of linear and nonlinear stiffness terms (i.e. ω_1 and ω_3, respectively) was used. All the curves have well known bent resonance shape with a region where multiple solutions are possible for a single forcing amplitude and frequency. For some sets of the parameters ω_1 and ω_3 this multi-valued solution region extends over a larger range of frequency than for others. When the linear stiffness is increased, the whole resonance peak shifts to higher frequencies. For example, the base of the curve shown with a solid line(i.e. $\omega_1 = 1$, $\omega_3 = 0.5$) seems to originate near 1 rad/s. When the linear stiffness is increased to $\omega_1 = 2$ the resonance shifts upward, as shown by the curve with open circles. When the linear stiffness is held constant and the nonlinear stiffness is varied, the shape of the peak changes. For example, the curve with a dashed line is for $\omega_3 = 0.25$, and is seen to bend less severely than the curve for $\omega_3 = 0.5$.
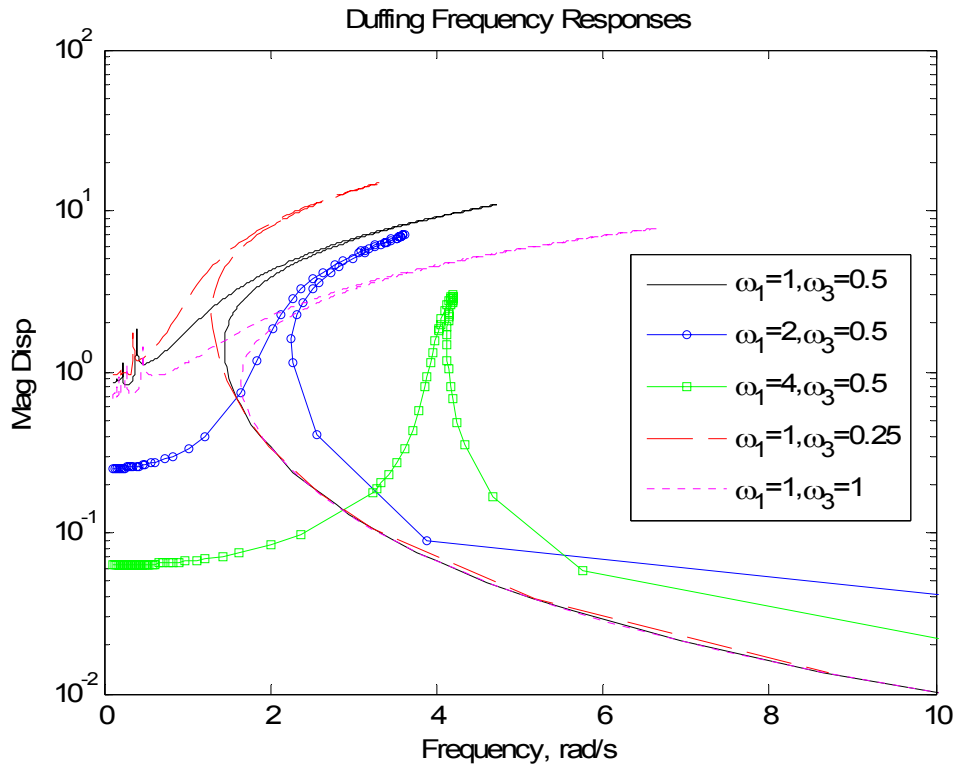
Fig. 2 Frequency response curves of the Duffing system for different linear (ω_1) and nonlinear (ω_3) stiffness values

Figure 2 also shows that the linear and nonlinear stiffness terms have coupled effects on the shape of the shape of the nonlinear FRF. For example, the shape of the frequency response curves can be seen to change when the linear stiffness is varied, even though the nonlinear stiffness term is held constant at $\omega_3 = 0.5$. Furthermore, none of the curves in the figure has the same peak magnitude, even thought the forcing amplitude was the same in all cases (i.e. it was equal to 1 in all cases). Nevertheless, the nonlinear frequency response curves do change in a fairly straightforward way so it would appear that, given a reasonable set of measurements, one could adjust the system model until it has the same frequency response as the measurement. The dynamics of higher order nonlinear systems can be more complicated, but they often show this same characteristic shape and hence these same principles could be used to tune a model until it reproduces each resonance accurately.

5. Nonlinear cantilever beam system

In a few recent papers, the Sracic and Allen have worked with a cantilever beam that has a geometric nonlinearity at its free end [14, 15]. Figure 3 below shows a top view photograph of the actual experimental setup. An aluminum 6061 alloy beam is bolted to a fixture that approximates a fixed base. A small strip of nylon is bolted to the free end of the cantilever and clamped to the fixture. The beam is oriented such that the bending axis is parallel to the plane of the table top. Figure 4 shows a close top and front view of the nylon strip that is clamped between the tip of the beam and the right hand side support. Table 1 below provides the physical dimensions of the beam and the nylon strip in millimeters.
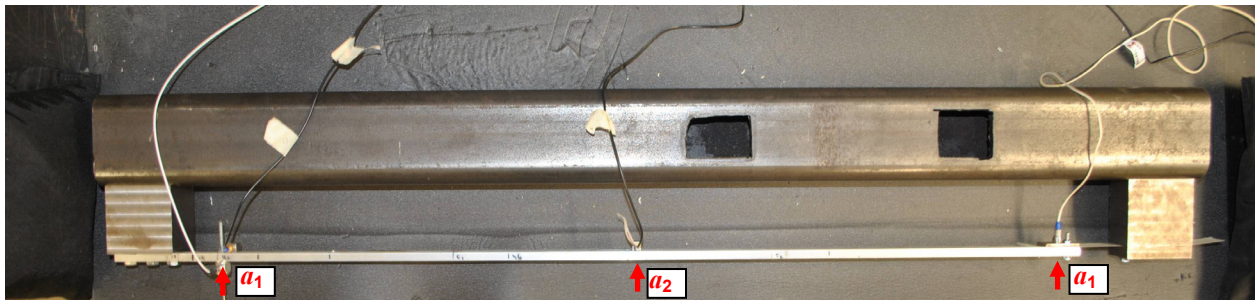
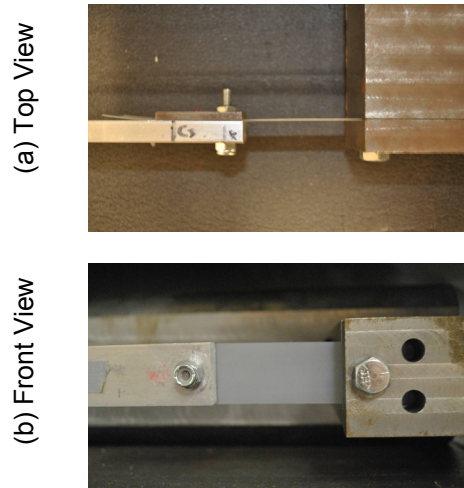**Fig. 3** Top view of the experimental nonlinear beam setup

(a) Top View

(b) Front View

Fig. 4 Top view (a) and front view (b) of the spring steel connected to free end of the cantilever beam

Table 1 Dimensions, in millimeters, of the 6061 Aluminum beam and the nylon strip, and the location of measurement sensors from the approximated fixed end

Dimension	Al 6061 Beam	Nylon 6/6 Strip	Sensor Location
Length	1016	53.2	a_1=45
Width	25.4	25.4	a_2=508
Thickness	9.5	0.254	a_3=984

The nylon strip at the tip of the beam adds stiffness at that point that depends nonlinearly on the tip displacement. This setup was originally proposed in [16], although their beam had a strip of spring steel instead of nylon, and other researchers have studied similar beam setups [17-19].

An analytical model of this system was created, as described in the schematic in Fig. 5. The beam is modeled as a uniform, prismatic cantilever beam with material density ρ, elastic modulus E_b, cross sectional area A_b, bending area moment of inertia I, and length L. The position along the length of the beam is given by the variable 'x'. The deflection of the beam is designated with the variable y. The beam has a nonlinear spring at its tip with stiffness k_{nl}. The equations of motion of the analytical beam are derived in Appendix 1.

$$F_{ext} = A_{ext} \sin(\omega_T t)$$

x

y

DOF 1   DOF 2   DOF 3

ρ, E_b, A_b, I, L
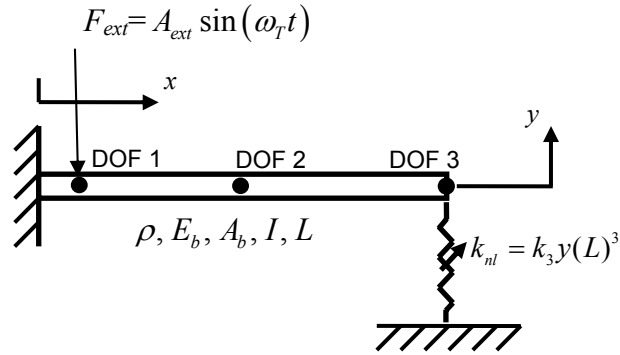
$k_{nl} = k_3 y(L)^3$

Fig. 5 Schematic of the nonlinear beam

In order to mimic the experimental system, the following parameters were used for the original model, which are based on the nominal properties of the experimental hardware: ρ=2700 kg/m^3, E_b=68GPa, A_b=3.23*10^{-4} m^2, I = 4.34*10^{-9} m^4, L = 1.016 m. Using these properties with the Ritz-Galerkin method, the two linear natural frequencies of the system are $\omega_1/(2\pi)$= 9.97 Hz and $\omega_2/(2\pi)$=62.51 Hz. Modal damping was added to the model assuming a coefficient of critical damping of ζ=0.01 for all modes. The transverse stiffness of the nylon strip is approximated in the model as $k_3 = E_n A_n / (2 l_n^3)$, where E_n, A_n, and l_n are the elastic modulus, cross sectional area, and length of the nylon strip. For the original model, the nylon was assumed to have an elastic modulus of E_n=3.9 GPa, which makes the nonlinear stiffness k_3= 8.75*10^7 N/m^3. A derivation of this approximation can be found in the appendix in [14], although in that work spring steel was used at the beam's free end instead of nylon.

The experiment was designed to produce a cubic nonlinearity. However, several practical design aspects could lead to other forms of nonlinearity in the response. For example, Fig. 4(a) shows that the nylon strip is offset from the neutral bending axis of the beam, which has the potential to produce a quadratic nonlinear contribution to the response. Additionally, the fixed end of the cantilever is realized using bolts, and the effective length of the beam may change depending on the direction of the deflection. The finite order model of the beam was developed assuming a perfect cantilever and a perfectly cubic spring at the beam's free end. Therefore, the goal is to use the frequency responses to improve the model so that it more closely represents the actual beam.

5.1   Frequency Responses of the Nonlinear Beam

The procedure described in Section 3 was used to measure the periodic responses of the nonlinear beam in order to calculate the beam's frequency responses. Harmonic excitation was applied to the beam with a model 2100E11-100 lb Modal Shaker from The Modal Shop, Inc. The beam was approximated as a having a fixed support, so the shaker was freely hung from a lateral excitation stand, as recommended in [20]. A thin steel stinger was used to transmit the excitation from the shaker to the beam. One end of the stinger was clamped inside the shaker armature and the other end was fixed to a force transducer, model 208C04 from PCB Piezotronics, Inc. (PCB), which was bolted to the beam at a location x = 45 mm from the fixed end of the beam. Harmonic forcing was provided by the National Instruments PXI system described in Section 3. The peak force amplitude, which was measured by the force transducer, was 70 N.. The response was measured with two Endevco model 66A12 triaxial accelerometers (only the z-channels were used) located at x = 45 mm (DOF 1; shaker location) and x = 508 mm (DOF 2; beam center) and with an Edevco model 256-100 isotron accelerometer located near the free end of the beam at x = 984 mm (DOF 3; beam tip). The degree-of-freedom locations are labeled with arrows in Figure 3. All of the accelerometers were secured to the beam with wax.

Initially, a fast sweep was performed using a large step size (frequency increment) in order to estimate the resonance frequencies. The first three resonances were found to be near 14, 45, and 120 Hz. The program was then set to automatically perform forward and backward frequency sweeps using a variable step size. Specifically, a step size of 0.1 Hz was used near the resonances and 0.5Hz in the regions away from the resonances. This approach decreased the testing time significantly while still capturing all of the features of the nonlinear frequency response accurately.

After the measurements were obtained, the method described in Section 2.1 was used to calculate each point on the frequency response curve from the measured periodic responses. In particular, the spectra of the measured accelerations were calculated with the Fast Fourier Transform, and the amplitudes of all the harmonic peaks were collected (since the steady-state response is periodic, these are the coefficients of the Fourier Series description of the response). In order to estimate displacement, each harmonic peak was integrated twice by dividing frequency squared. Then, the displacement amplitudes of all the harmonics were summed to give the estimate for the magnitude of displacement.

Next, the frequency response of the model beam was calculated with the numerical continuation technique. The algorithm was set to find the nonlinear frequency response between 2 and 150 Hz. For each periodic response, the instant at which the displacement of DOF 3 (i.e. the tip displacement) was maximum was found and recorded, and the displacements of the other DOF were recorded at the same instant. These amplitudes were used to plot the magnitude of the frequency response. Note that this assumes that all the degrees-of-freedom reach their extreme displacement at the same instant, which may not be the case for very nonlinear systems or for when there are complicated modal interactions. However, it will be shown that the accuracy of the model can still be inferred using this approach.

Figure 6 shows the frequency response functions that were calculated from the measurements of the beam as well from the numerical continuation simulations. The dashed curves with markers show the results from the experiment (open blue squares-accelerometer a_1, open green circles-accelerometer a_2, red dots-accelerometer a_3). The solid lines are the frequency response curves that were calculated with the numerical continuation technique (blue-DOF 1, green-DOF 2, red-DOF 3). There are three dominant resonance peaks in most of the curves except for the DOF 2 curves (green). The first two resonance peaks in the model curves occur near 10 and 47 Hz and are bent to higher frequencies, while the third peak near 130 Hz appears to be predominantly linear. In the curves from the experiment, the first two peaks occur near 14 and 44 Hz. They seem to have a bent shape, but when they reach a certain frequency the curve sharply drops in magnitude, which many would recognize as the well know jump-phenomenon for the multi-valued region (i.e. the response jumps from a large amplitude periodic response to a small one). Additionally, the first resonance of the model seems to bend more significantly than the curves from the experiment and the curves from the model contain several superharmonic resonances below 5 Hz. This range was not tested in the experiment because the freely suspended shaker moved quite a bit in that frequency range causing the measurements to be unreliable. Lastly, the amplitude of the resonance peaks in the model's responses for DOF 1 (i.e. the blue curve, especially for the peaks near 47 and 130 Hz) appear to be much smaller than those of the actual system.
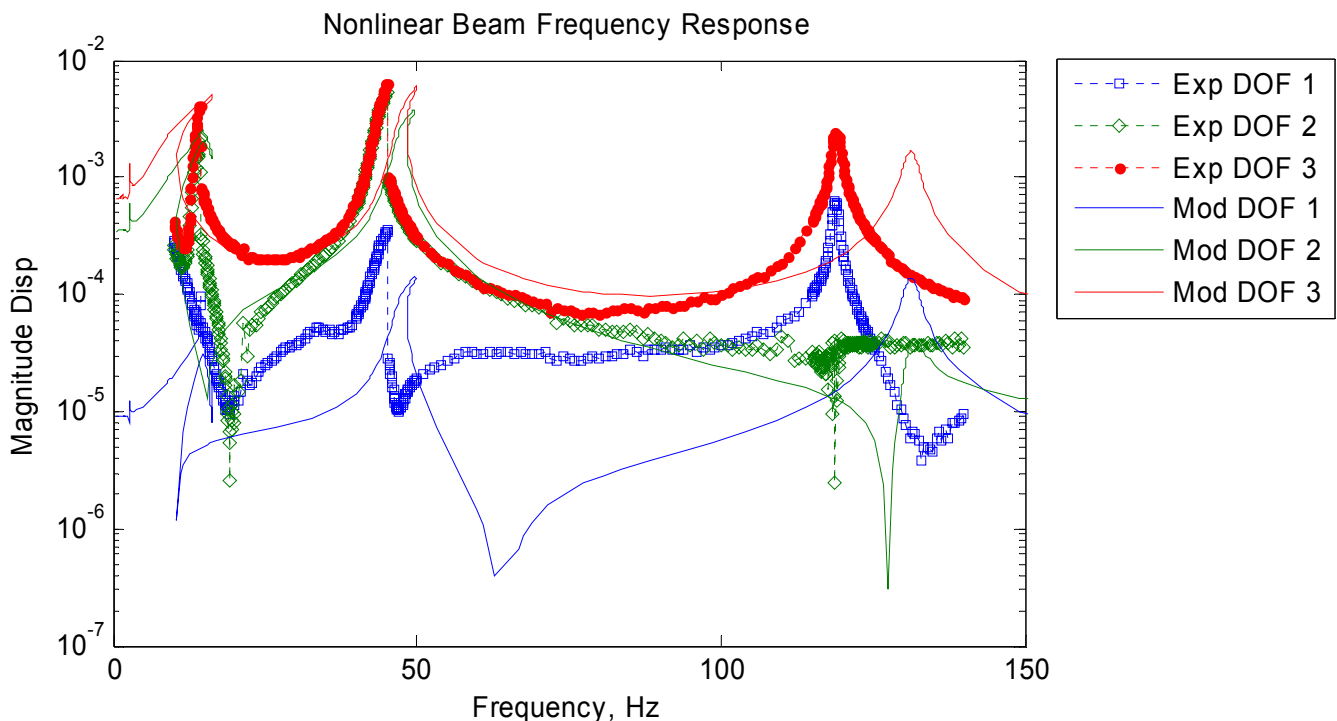

Nonlinear Beam Frequency Response

Fig. 6 Comparison #1 of frequency response curves for the experiment (Exp) and the model (Mod) for model parameters: E_b=68GPa, E_n=3.9 GPa, k_3= 8.75*10^7 N/m^3

The frequency response curves show that the model accurately characterizes the number of modes in this frequency band of interest, and the fact that the nonlinearity is most apparent in the first and second modes. However, there are several significant discrepancies. The amplitude of the peaks in the model's curve for DOF 1 are too small, indicating that this DOF's amplitude is smaller than the actual hardware. This discrepancy may arise because the model has a perfect fixed base, while the fixture in the experiment has finite compliance. Another important issue is that the frequencies where the resonances occur differ between the model and the actual beam. The frequencies of the second two modes are too high in the model. As in the single degree-of-freedom case, this property is influenced by the linear stiffness of the system. Therefore, the elastic modulus of the beam can be reduced to decrease the linear stiffness and hence the frequency of all the resonance peaks. Figure 7 shows the second comparison between the measured frequency responses and those from the model after reducing the elastic modulus of the beam to E_b=55.5GPa (note that this value is still in the nominal range for the aluminum). No other parameters in the model were changed.

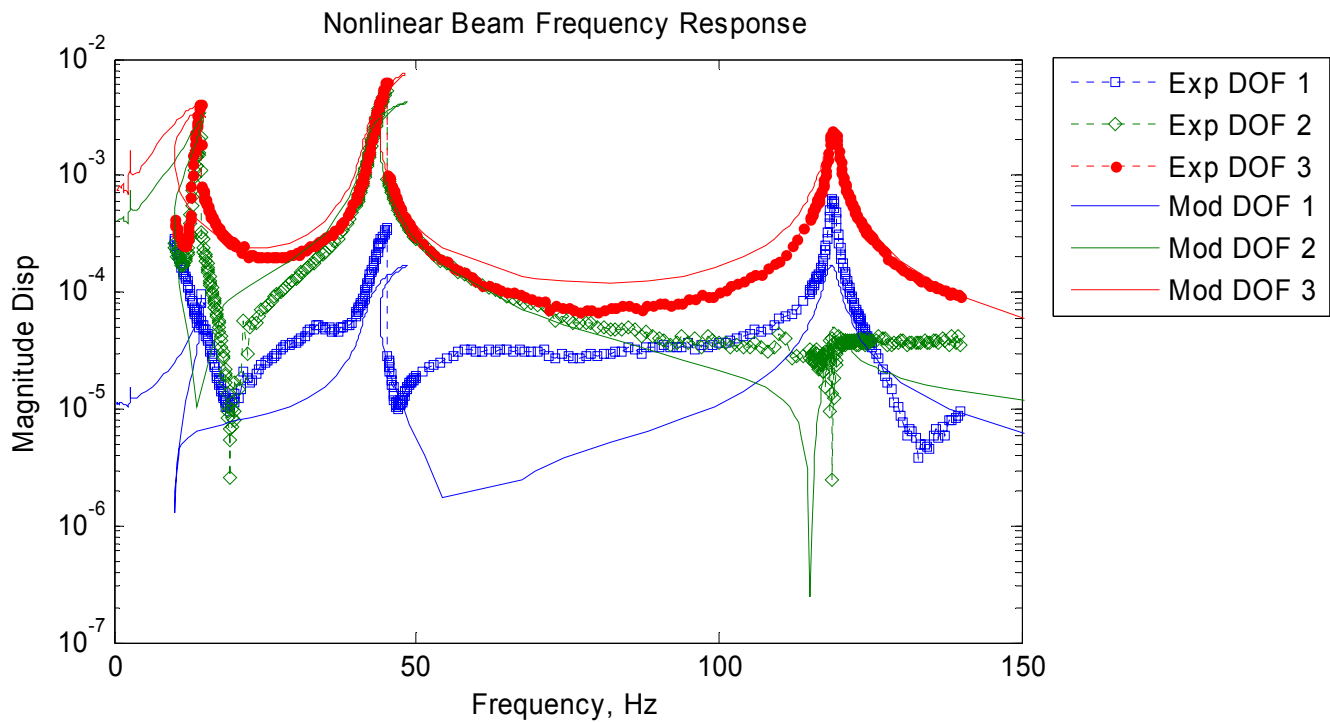**Fig. 7** Comparison #2 of frequency response curves for the experiment (Exp) and the model (Mod) for model parameters: E_b=55.5GPa, E_n=3.9 GPa, k_3= 8.75*10^7 N/m^3

With a lower elastic modulus, the location of the resonance peaks has changed to be more in line with the measurements, but the shapes of the peaks has changed as well. The resonance of the third mode near 119 Hz seems to align very well with the measurements, and the peaks seem to have the same magnitude except for DOF 1. The model's second resonance peak also seems to align more closely with the measurements. However the peaks in the simulated frequency responses bend over more than the measurements and more than they did in Fig. 6. This is evidence that the linear and the nonlinear stiffness of the model are coupled, since only the linear stiffness was changed but a nonlinear feature of the second resonance also changed. The same seems to be true for the first resonance. However, one must use caution when comparing the simulated frequency responses with the measurements, since the actual beam may have jumped to a lower amplitude response before reaching the absolute peak of the frequency response curve. The phase of the response can be used to investigate this, since the phase should be 90 degrees at the extreme of the resonance curve. The phase of the response was calculated at the jump frequency for the resonance near 14 Hz by computing the difference

between the phase of the fundamental harmonic of the response and the fundamental harmonic of the force. For DOF 3 at 14.3 Hz the phase difference was found to be -83.26 degrees, suggesting that the experiment captured nearly the full nonlinear resonance curve for DOF 3 before the jump happened. In contrast, the phase of DOF 3 at the 45.11 Hz jump frequency was 74.86 degrees, revealing that portion of the second resonance curve was probably missed in the experiment. However, the peaks in the model's responses still seem to bend over larger frequency ranges than those of the actual beam suggesting that the nonlinear stiffness of the model is too large. Hence, the model was updated again by reducing the modulus of the nylon spring to E_n=0.24 GPa, which yields a nonlinear stiffness coefficient of k_3= 5.38*10^6 N/m^3. The frequency responses of the model were recomputed and are shown in Fig. 8. This has caused the shape of the model's resonances to change so that the first two resonances do not bend as much towards higher frequencies. Unfortunately, the peaks near 44 Hz now do not seem to bend as much as those in the measurements. The peaks near 12 Hz have a larger maximum magnitude than the previous case and yet they still seem to bend more than those in the measurements. It also seems apparent now that the model's resonance curves are centered at a significantly lower frequency than those in the measurements.
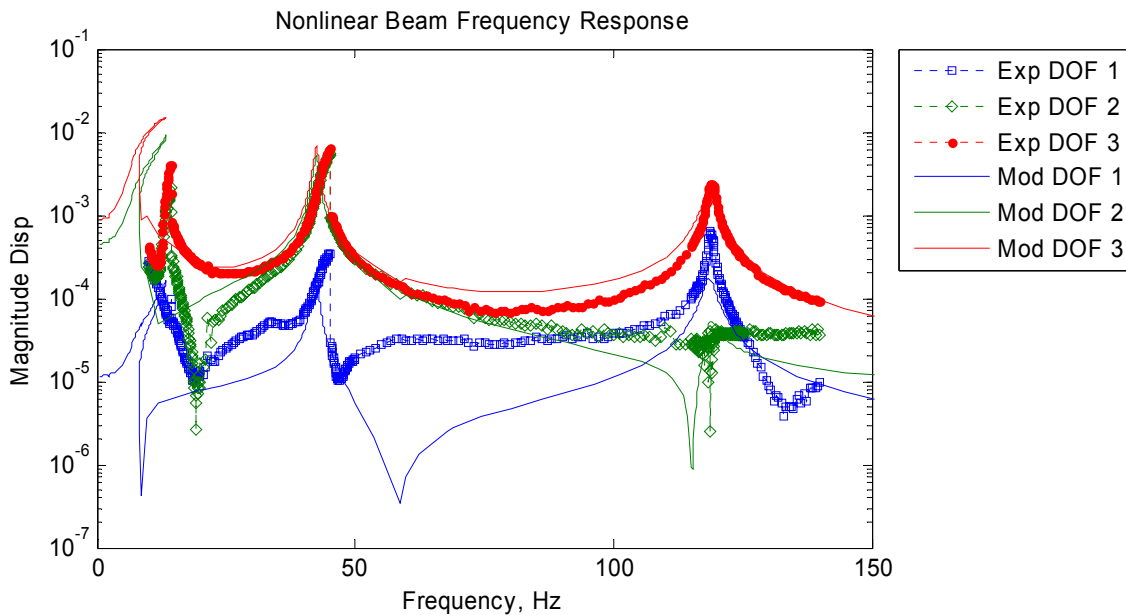

Fig. 8 Comparison #3 of frequency response curves for the experiment (Exp) and the model (Mod) for model parameters: E_b=55.5GPa, E_n=0.24 GPa, k_3= 5.38*10^6 N/m^3

5.1.1   Discussion

By simply adjusting the modulus of the beam (i.e. in Fig. 7), the nonlinear frequency responses of the model were made to agree much more closely with the actual measurements, at least for the second and third resonances. The shape of the resonance curve for the second mode was also improved as well. However, the linear and nonlinear stiffness terms have a coupled effect on the nonlinear FRFs so it was not trivial to bring the first mode into agreement nor to match the shape of that resonance. It is likely that the current beam model cannot be updated to agree more closely with the measurements without relaxing certain assumptions in the model. For example, it may be important to consider the finite stiffness of the support at the base of the cantilever, rather than treating it as a fixed support. Likewise, the nylon strip may actually impart a linear stiffness to the beam tip and the mass of the bolts, accelerometers and/or load cell may be significant.

By construction, the methods in this paper can also be used to validate the terms that are used to describe the nonlinearity. For example, Fig. 9 shows the Fourier coefficients of the estimated displacement response of the actual beam for the first resonance. The coefficients of the first three harmonics (i.e. m=1, 2, and 3) are shown in subplots (a), (b), and (c), respectively. The degrees-of-freedom are shown with open squares (DOF 1), open diamonds (DOF 2), and dots (DOF 3). Recall that for a linear system only the coefficients in 9a would be nonzero. Hence, by viewing the responses in this way one can see that the first resonance is dominated by the m=1 and m=3 responses, while the m=2 harmonic is significantly weaker. Other harmonics are present but are not shown.)
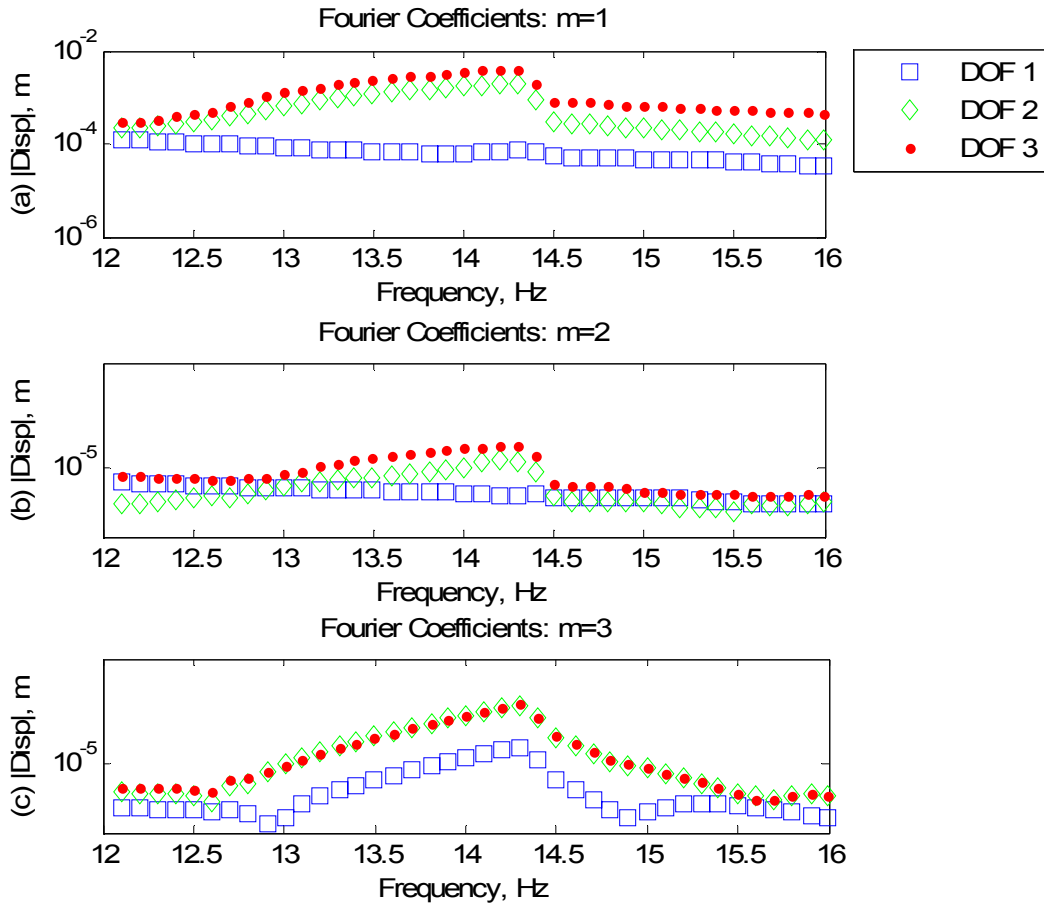
Fig. 9 Fourier coefficients of the actual beam's steady state forced response, extracted during the nonlinear frequency response calculation. The first three harmonics are shown in (a), (b), and (c).

The harmonics in the response provide information on the type of nonlinearity that is present in the system. In particular, the m=3 harmonic is associated with a cubic nonlinearity., The presence of a m=2 harmonic could be due to the existence of a quadratic type nonlinearity in the system. So, one could continue to interrogate the harmonics of the responses to see what terms provide a contribution, and ideally the responses of the model should also contain these harmonic terms. The model in this paper was not designed with any quadratic

nonlinear terms, but these observations suggest that a term of the form $k_2 y(L)^2 * \begin{bmatrix} \psi_1(L) & \cdots & \psi_N(L) \end{bmatrix}^{\mathrm{T}}$ should

be inserted into the equations of motion in Appendix 1.

6. Conclusions

This paper has explored model updating for nonlinear systems by measuring the nonlinear frequency response of the system and comparing those with the simulated frequency responses of a representative model. The experiment was performed with a controlled stepped-sine test that measures the steady state, periodic response of the nonlinear system at each forcing frequency. Then, the measured time histories can be processed to display the nonlinear frequency response over a range of forcing frequencies. The nonlinear frequency response of the system model was found using a numerical continuation technique. The algorithm employed a Newton-Raphson shooting and updating technique and finite differences gradients so that the closed form equations of motion were not needed. One advantage of this approach is that the time histories used by this algorithm could be supplied by a finite element analysis package, simplifying the modeling process. The frequency responses contain many characteristics that are similar to linear frequency response functions (e.g. resonance peaks that are related to the modes of the system), so many of the same principles from linear modal analysis can be used

to evaluate and update the system model. In addition, the nonlinear characteristics of these curves (e.g. the shape of bent resonance peaks), can be used to validate the nonlinear parameters of the model.

This approach was evaluated using an actual cantilever beam with a geometric nonlinearity at its tip. The beam's nonlinear frequency responses were measured (up to the limits of the modal shaker) and nonlinearity was clearly observed. A simple Ritz-Galerkin model of the beam was created and its parameters were adjusted to more closely reproduce the three measured resonance peaks. The locations of the resonance peaks were used to update the linear stiffness of the model, which brought the model and measurements into much closer agreement. On the other hand, the model had difficulty reproducing the shapes of the first two resonance curves for any value of the model parameters. The results suggest that other features of the model must be adjusted to obtain better agreement. For example, the response of the beam was interrogated, revealing that a weak quadratic term was present and should be added to the beam model in order to more faithfully reproduce the response.

7. Appendix 1 Ritz-Galerkin Discrete Model

A Galerkin approach was used to create a finite-order model of the experimental structure. Assuming that the beam behaves linear-elastically, mode shapes corresponding to transverse bending motion were used as shape functions to construct the Ritz-Galerkin representation [21]. The displacement of the beam at a position x was approximated as

$$y(x,t) = \sum_{r=1}^{N_m} \psi_r(x) q_r(t) \tag{7}$$

where $\psi_r(x)$ is the rth Euler-Bernoulli beam mode shape for a cantilever, $q_r(t)$ is the rth generalized coordinate, and N_m is the number of modes used. The system's undamped equations of motion are provided in the following equation, where the coordinates are the amplitudes of the basis functions.

$$\rho A_b L [M] \ddot{q} + \frac{E_b I}{L^3} [K] q = Q = \sum f_{ext} \psi_r(x_f) \tag{8}$$

For the generalized coordinates, a time derivative is denoted with an over-dot (e.g. the generalized acceleration vector is $\ddot{q}$). Modal damping was added to the system by performing an eigenvector analysis on the linear system and then using,

$$[C] = (\rho A_b L)^2 [M][\phi_b][diag(2\zeta_r \omega_r)][\phi_b]^{\mathrm{T}}[M] \tag{9}$$

where $[\phi_b]$ is a matrix containing the eigenvectors in the columns, ω_r is the rth circular natural frequency, and ζ_r is the rth desired damping ratio. The generalized force vector Q is a sum of the product between all external forces and the value of the shape functions at the point where the force is applied, x_f. Therefore, Q includes the applied or external forces, F_{ext} in Fig. 5, as well as the nonlinear restoring force due to the spring [21]. The beam provides linear stiffness at the tip due to its flexural rigidity, so the discrete spring's stiffness was chosen to be purely nonlinear

$$k_{nl} = k_3 y(L)^2 \tag{10}$$

where k_3 is a stiffness constant associated with the nonlinear spring. The physical restoring force due to the spring is then equal to $f_{sp} = k_3 y(L)^3$. The generalized force vector then has components corresponding to the nonlinear spring located at $x=L$ and the externally applied force located at $x=x_f$.

$$\{Q\} = k_3 y(L)^3 \begin{Bmatrix} \psi_1(L) \\ \vdots \\ \psi_N(L) \end{Bmatrix} + A_{ext} \sin(\omega_T t) \begin{Bmatrix} \psi_1(x_f) \\ \vdots \\ \psi_N(x_f) \end{Bmatrix} \qquad (11)$$

A_{ext} is the amplitude and ω_T the frequency of the external forcing term that produces the limit cycle.

After using the Ritz-Galerkin method to form the discrete beam model and to account for the nonlinear applied force of the spring, the equations of motion were transformed back into physical coordinates using the relationship in Eq. (7). The differential equations of motion can then be arranged in state space format.

$$\begin{Bmatrix} \dot{y} \\ \ddot{y} \end{Bmatrix} = \begin{Bmatrix} \dot{y} \\ -[M_p]^{-1}\left([C_p]\dot{y} + [K_p]y + \{F\}\right) \end{Bmatrix}$$

$$[M_p] = \rho A_b L [\Psi]^{-T}[M][\Psi]^{-1}, \quad [C_p] = [\Psi]^{-T}[C][\Psi]^{-1}, \qquad (12)$$

$$[K_p] = \frac{E_b I}{L^3}[\Psi]^{-T}[K][\Psi]^{-1}, \quad \{F\} = [\Psi]^{-T}\{Q\}$$

The matrix $[\Psi]$ has the numerical values of the mode vectors for specific position coordinates on the beam. Then, $[\Psi]$ can contain shape functions evaluated at the nodal degrees of freedom on the beam. In this study the number of mode shapes used in the expansion and the number of degrees of measurement points (shown in Fig. 5) was $N = N_m = 3$. The nodes were located at the center and tip of the beam as shown in Fig. 5.

References

[1]   T. C. Kim*, et al.*, "Super- and Sub-Harmonic Response Calculations for a Torsional System with Clearance Nonlinearity Using the Harmonic Balance Method," *Journal of Sound and Vibration,* vol. 281, pp. 965-993, 2005.
[2]   H. A. DeSmidt, "Analysis of a Dual Gearbox/Shaft System with Nonlinear Dynamic Mesh Phase Interactions," presented at the 51st AIAA/ASME/ASCE/AHS/ASC Structures, Structural Dynamics and Materials Conference, Orlando, Florida, USA, 2010.
[3]   C. Padmanabhan and R. Singh, "Analysis of Periodically Excited Non-linear Systems by a Parametric Continuation Technique," *Journal of Sound and Vibration,* vol. 184, pp. 35-58, 1995.
[4]   P. Ribeiro, "Non-linear Forced Vibrations of Thin/Thick Beams and Plates by the Finite Element and Shooting Methods," *Computers and Structures,* vol. 82, pp. 1413-1423, 2004.
[5]   A. H. Nayfeh and D. T. Mook, *Nonlinear Oscillations*. New York: John Wiley and Sons, 1979.
[6]   C. Gibert, "Fitting Measured Frequency Response Using Non-Linear Modes," *Mechanical Systems and Signal Processing,* vol. 17, pp. 211-218, 2003.
[7]   M. W. Sracic and M. S. Allen, "Numerical Continuation of Periodic Orbits for Harmonically Forced Nonlinear Systems," presented at the 29th International Modal Analysis Conference (IMAC XXIX), Jacksonville, Florida, USA, 2011.
[8]   M. Peeters*, et al.*, "Nonlinear Normal Modes, Part II: Towards a Practical Computation Using Numerical Continuation Techniques," *Mechanical Systems and Signal Processing,* vol. 23, pp. 195-216, 2009.
[9]   A. Carrella and D. J. Ewins, "Identifying and Quantifying Structural Nonlinearities in Engineering Applications From Measured Frequency Response Functions," *Mechanical Systems and Signal Processing,* vol. 25, pp. 1011-1027, 2011.
[10]   M. Imregun*, et al.*, "Finite Element Model Updating Using Frequency Response Function Data: I. Theory and Initial Investigation," *Mechanical Systems and Signal Processing,* vol. 9, pp. 187-202, 1995.
[11]   J. Guckenheimer and P. Holmes, *Nonlinear Oscillations, Dynamical Systems, and Bifurcations of Vector Fields* vol. 42. New York: Springer-Verlag New York Inc., 1983.

[12] G. Kerschen, Peeters, M., Golinval, J.C., Vakakis, A.F., "Nonlinear Normal Modes, Part I: A Useful Framework for the Structural Dynamicist," *Mechanical Systems and Signal Processing,* vol. 23, pp. 170-194, 2009.

[13] M. W. Sracic, "A New Experimental Method for Nonlinear System Identification Based on Linear Time Periodic Approximations," Ph.D. Engineering Mechanics, Department of Engineering Physics, University of Wisconsin-Madison, Madison, 2011.

[14] M. W. Sracic and M. S. Allen, "Identifying parameters of nonlinear structural dynamic systems using linear time-periodic approximations," presented at the 29th International Modal Analysis Conference (IMAC XXIX), Jacksonville, Florida, USA, 2011.

[15] M. W. Sracic and M. S. Allen, "Identifying parameters of multi-degree-of-freedom nonlinear structural dynamic systems using linear time periodic approximations," *Mechanical Systems and Signal Processing,* (Submitted July 2011).

[16] F. Thouverez, "Presentation of the ECL Benchmark," *Mechanical Systems and Signal Processing,* vol. 17, pp. 195-202, 2003.

[17] G. Kerschen, Lenaerts, V., Golinval, J.C., "Identification of a Continuous Structure with a Geometrical Non-Linearity. Part I: Conditioned Reverse Path Method," *Journal of Sound and Vibration,* vol. 262, pp. 889-906, 2003.

[18] G. Kerschen*, et al.*, "Past, Present and Future of Nonlinear System Identification in Structural Dynamics," *Mechanical Systems and Signal Processing,* vol. 20, pp. 505-592, 2006.

[19] K. Worden and G. R. Tomlinson, "A Review of Nonlinear Dynamics Applications to Structural Health Monitoring," *Strucrural Control and Health Monitoring,* vol. 15, pp. 540-567, 2007.

[20] R. L. Mayes and A. J. Gomez. (2006) What's Shakin', Dude? Effective Use of Modal Shakers. *Experimental Techniques*. 51-61.

[21] J. H. Ginsberg, *Mechanical and Structural Vibrations Theory and Applications*, 1 ed. New York: John Wiley & Sons, Inc., 2001.